Predicting network congestion by extending betweenness centrality to interacting agents

Marco Cogoni and Giovanni Busonera
CRS4 Center for Advanced Studies, Research and Development in Sardinia - Via Ampere 2, 09134 Cagliari (CA) Italy

(Received 30 November 2023; accepted 22 January 2024; published 3 April 2024)

We present a simple model to predict network activity at the edge level by extending a known approximation method to compute betweenness centrality with a repulsive mechanism to prevent unphysical densities. By taking into account the strong interaction effects often observed in real phenomena, we aim to obtain an improved measure of edge usage during rush hours as traffic congestion patterns emerge in urban networks. In this approach, the network is iteratively populated by agents following dynamically evolving fastest paths who are progressively attracted towards uncongested parts of the network as the global traffic volume increases. Following the transition of the network state from empty to saturated, we study the emergence of congestion and the progressive disruption of global connectivity due to a relatively small fraction of crowded edges. We assess the predictive power of our model by comparing the speed distribution against a large experimental data set for the London area with remarkable results, which also translate into a qualitative similarity of the congestion maps. Also, percolation analysis confirms the quantitative agreement of the model with the real data for London. We perform simulations for seven other topologically different cities to obtain the Fisher critical exponent τ that shows no common functional dependence on the traffic level. The critical exponent γ, studied to assess the power-law decay of spatial correlation, is found to be inversely proportional to the number of vehicles for both real and simulated traffic. This simulation approach seems particularly fit to describe qualitative and quantitative properties of the network loading process, culminating in peak-hour congestion, by using only topological and geographical network features.

DOI: 10.1103/PhysRevE.109.044302

I. INTRODUCTION

One of the networking metrics that have been used the most in recent years to analyze network behavior is the betweenness centrality (BC). This measure of relative importance among the constituents of a network during a simultaneous peer-to-peer linkage process originated in the study of relations among people and abstract ideas [1], but it has been applied with some success to transportation infrastructures such as airlines, cargo ships, power grids, and computer networks [2–5]. It is roughly defined as the total flow passing over each node of a network when enumerating all origin-destination (OD) pairs and connecting them via shortest paths. The definition of BC is easily extended to edges by measuring edge usage instead of nodes and we will refer to this variant throughout the paper [6]. A major limitation of standard centrality-based approaches is that they can often grasp only a limited picture of a real network under stress [3,5]. This is due to the fact that they rely on two main assumptions [7,8]: (i) Edge usage has fixed costs and (ii) unlimited agents can share the transport infrastructure regardless of physical capacity [9]. Betweenness centrality and other centrality measures have been used to predict which edges are subject to the highest traffic demand, but the correlation with simulated or real traffic tends to vanish in the high-density regime [3] and in the presence of phenomena that are not explainable just with geographical or topological features [4]. Edge usage obtained from BC in fact typically mimics a low-density state of the network that usually happens with very small (compared to network geography) or very fast (with respect to congestion buildup timescales) agents [5].

In this work we aim to improve upon the standard BC by taking into account the strong interaction effects observed in real networks, in order to obtain a better measure of edge congestion. Our method will be developed for urban transportation, using an approach that is easily transferable to other contexts [10–13]. The limited capacity of transportation infrastructures was previously considered in Ref. [14], which focused on the price of anarchy in urban networks, and in Ref. [15], whose main goal was to develop an accurate sociodemographic model to generate origin-destination pairs. Both works implemented very simple traffic models and did not consider the order of vehicle addition or dynamic fastest path recalculation.

Urban networks have been widely studied in recent years [13,16,17], in terms of both their growth over time and their complex dynamics for different traffic levels. Network science has considerably helped to improve our understanding of cities and to analyze and predict the reaction of the different parts of the network under stress [11]. Such predictive analyses may be performed by using models depending just on the geographical and topological features of a city, avoiding experimental traffic data, after careful validation against observations [18,19]. Urban networks belong to the special class of (almost) planar graphs [20,21] whose topology is constrained by the geographical embedding. This severely hinders their long-range connectivity and also limits their maximum node degree [22]. Since the study of node degree distributions alone cannot be expected to significantly improve our understanding of cities, nonlocal higher-order metrics such as network centralities have been widely used both for

theoretical studies and for practical applications with notable success [1,23].

In this article (Sec. II) we present a method where agents iteratively populate the network along dynamically evolving fastest paths. These paths are gradually pushed towards uncongested areas of the network as global traffic volume rises. We examine the transition of the network state from empty to saturated, investigating the emergence of congestion and the gradual disruption of global connectivity caused by a relatively small fraction of crowded edges. Since it is still an open question how people plan their routes when driving in urban networks, but given that a growing fraction of drivers use some form of dynamic routing help, our moving agents will be modeled as a population of selfish drivers [14], thus representing any mix of self-driving cars and humans using real-time traffic information. In this context, our results (Sec. III) that compare synthetic and real data show remarkable improvements with respect to standard BC: Whole network speed distributions agree quantitatively and spatial patterns of congestion are qualitatively very similar. The qualitative comparison is supported by an analysis of how the spatial correlation of congestion decays with distance (measured as the travel time on an empty network). Percolation analysis also produces compatible results for critical exponents within different traffic conditions.

II. METHODS

In real urban networks, the average travel time is of the same order of magnitude as the typical timescale of congestion buildup. The strength of the interaction among vehicles depends on their local density and on the duration of the network loading process during rush hour: Slower vehicles stay on edges longer, so their occurrence probability in a given road segment during the observation period is larger. Our approach stems directly from this fact and also takes into account that peak-hour periods are limited in time, usually lasting about one hour [16]. This allows estimating the cumulative traffic seen on the roads during that finite time window. Thus, we propose a pseudodynamical model taking into account the contribution to traffic at a road-segment level due to each vehicle added to the network, by updating travel times at each step. The approach could in principle be extended to model the congestion decay that occurs when traffic volume eventually decreases, by removing vehicles reaching their destinations.

From the vast literature on transportation, we choose one of the simplest models to describe vehicular behavior depending on the edge physical properties and on the dynamical network state, the single-regime Greenshields model [21,24], for which speed starts as free flow on an empty road, decreasing linearly to zero with maximum density. To complement the traffic model, we impose a selfish behavior on our vehicles: They follow the fastest path (not the shortest one) as computed at the time of leaving their origin node.

A. Interaction model

We simulate the network evolution, as observed by travelers, while the traffic increases from zero up to almost complete gridlock, signaled by the vanishing probability of adding new paths not containing congested edges. The traffic network is modeled as a directed, weighted graph whose edges, identified by e, represent road segments between adjacent intersections (nodes) and possess three constant features: physical length l_e, maximum speed v_e^*, and number of lanes c_e. Nodes are featureless.

The network traffic grows incrementally by activating one new path π^i at each simulation step i, in order to reach the desired target value at time T (the end of the simulation). Thus, i can be interpreted both as the current number of added paths and as a temporal marker within the sequence of OD pairs randomly generated for each simulation. This procedure mimics the well-known method of approximating BC [25]. For simplicity, and to be able to compare results with respect to the standard BC, traffic will be added uniformly to the network. It is however straightforward to adapt our procedure to any OD matrix.

The state of the network at each time step is defined by the temporal occupancy factors due to all vehicles added so far to each edge: $s_e^i = \sum_{j=1}^{i} \sigma_e^j$. The single-vehicle occupancy σ_e^i is defined as the ratio between the time (crudely approximated) spent on edge e and T,

$$\sigma_e^i = \min\left(\frac{T_e^i}{T}, 1\right), \tag{1}$$

where $T_e^i = \frac{l_e}{v_e^i}$, with v_e^i following a Greenshields linear law [26]

$$v_e^i = v_e^*\left(1 - \rho_e^{i-1}\right), \tag{2}$$

where

$$\rho_e^{i-1} = \frac{s_e^{i-1} L}{l_e c_e} \in [0, 1] \tag{3}$$

is the normalized vehicle density at the previous step, monotonically increasing with i; L is the average space occupied by one vehicle; and the denominator represents the edge capacity. A noninteracting system, obtained in the limit $L \to 0$, approaches the state s_e as computed with the standard BC. The approximate time to travel along π^i will be the sum over the edges $T_{\pi^i} = \sum_{e\in\pi^i} T_e^i$. The total occupancy due to a single vehicle is $\sum_{e\in\pi^i} \sigma_e^i \leqslant 1$ and will only reach 1 for a path π^i with total traveling time $T_\pi \geqslant T$.

In more detail, the state of the network is iteratively obtained $[s_e^i = f(s_e^{i-1})]$, starting with unused edges ($s_e^0 = 0$ and $T_e^1 = \frac{l_e}{v_e^*}$) and according to the following dynamic process.

(i) A pair of OD nodes is chosen, independently and uniformly at random, and the fastest path π^i connecting the nodes is computed, given the current travel times T_e^i.

(ii) Starting from the origin, we assign the respective shares of occupancy σ^i induced by π^i during T, to each edge $e \in \pi^i$:

$$s_e^i = s_e^{i-1} + \sigma_e^i. \tag{4}$$

Note that, as soon as the sum along π^i of the added T_e^i/T factors reaches 1 (travel time longer than the simulation), we skip the remaining edges until the destination, to avoid increasing by more than a unit the vehicle occupancy along π^i.

(iii) The v_e^{i+1} and T_e^{i+1} are updated according to Eqs. (1) and (2), using the new ρ_e^i value.

(iv) This process is iterated until the target total traffic is reached.

Intuitively, the occupancy factor induced by a vehicle over an edge e is proportional to the time the vehicle is supposed to spend on it (T_e/T), as forecast at its departure, and the sum over the whole path will be equal to unity (certainty of finding the vehicle within π during T) only when $T_\pi \geqslant T$. Since the initial vehicles find a nearly empty network, their fastest paths and travel times are virtually equivalent to the noninteracting case. With rising traffic, however, edges fill up and the previous fastest paths will disappear and less-used roads and residential neighborhoods will be chosen. Some edges will eventually reach maximum density and become congested. If the fastest route from the origin to the destination comprises a congested edge (i.e., the network is disconnected) we still choose to add the initial part of the path but skip all remaining edges from the first congested one. This allows us to model the backward propagation of traffic jams observed at high traffic volumes [12,27]. The order in which OD pairs are selected for adding vehicles to the network can lead to different states; thus multiple replicas of the system are simulated to verify the stability of the results. Replicas differ in the subset of OD pairs chosen, but no relevant differences in the average results were detected just by reshuffling the same subset of ODs.

B. Spatial correlation of congestion

To estimate the degree of spatial correlation of congestion between edges, we adapt the definition of correlation used in modeling collective behaviors [28,29]. We define

$$C(t) = \frac{1}{c_0} \frac{\sum_{ij} \langle \rho_i^* \rho_j^* \rangle \delta(t - t_{ij})}{\sum_{ij} \delta(t - t_{ij})}, \tag{5}$$

in which ρ^* can assume the value 0 or 1 whether below or above the congestion threshold, respectively; t_{ij} represents the fastest travel time between the two edges on the empty network; δ is a rectangular window function selecting times close to t_{ij}; and c_0 is a normalization factor. Angular brackets refer to the ensemble average over replicas, where replicas may be independent simulations with different OD pairs or multiple instances of real traffic states for the same time slot and weekday. In our analysis, we will disregard the normalization factor c_0 since our focus is on the power-law decay of spatial correlation, described by the γ exponent. We compute our correlations as a function of travel time rather than distance. Travel time on the empty network, in this context, is the preferred way to estimate proximity between edges, because Euclidean distance is known to lead to distortions, as it disregards connectivity. Moreover, we perform correlation analysis on raw speed values and not on their fluctuations [27], as opposed to some previous studies [29,30].

III. RESULTS AND DISCUSSION

In order to validate our approach, we first compare the traffic properties of a large-scale real-world data set with those obtained from our interacting network model. We show that, just by imposing a simplified repulsion mechanism among vehicle paths, the agreement with real data markedly improves with respect to the standard BC. The comparison is first performed between speed distributions over the whole network. Then, by correlating the speeds edge to edge, we identify the simulated traffic volume V best matching the real data at peak hours. Since speed depends on road usage (vehicle density), we also compare the congestion map obtained from BC and from our model against measured data, illustrating how the proposed method seems to be able to reproduce realistic congestion states for high-volume traffic situations. We also compute the spatial correlation for edge congestion to verify whether the γ critical exponent is comparable to previous results for different traffic levels. Since another property characterizing the network is the cluster-size distribution during critical percolation, which is known to follow a power law with exponent τ, we also study its value for increasing traffic volumes and compare it against the real traffic data set at different hours.

A. Comparison with real-world measurements

To understand how realistic the results produced by the present model are, we compare them against a large experimental data set provided by Uber [31]. The data set provides GPS tracks for taxi fleets in several metropolitan areas, but only the data for the city of London was used in this work, discarding the others for insufficient sampling. All road networks were obtained from OpenStreetMap (OSM) [32] by using the OSMNX library and downloaded in their latest state, except in the case of London, for which we matched the period of the recorded real traffic data set. The Uber movement data set contains data recorded for a high fraction of the street segments at hourly intervals for several years: We selected the first six months of 2019 to avoid spurious effects due to the pandemic. Speed values in the data set are always one-hour averages from multiple vehicles since single-vehicle data are not available due to privacy concerns. For our analyses, we define a speed factor for every edge in the network as the ratio between the hourly average speed and the maximum value ever observed in that edge during the whole period. Since speed data can be sparse especially during low traffic (see Supplemental Material [33], Fig. S1a) and roads typically consist of several segments, we also derived a spatially coarser data set with fewer missing values. This was done by averaging speed on multiple edges belonging to a single street at the same time. The use of this coarser data set will be specified in the results. Throughout the paper, we will focus on four specific times of the workday: peak hours 8–9 and 17–18 and off-peak hours 10–11 and 22–23. See Fig. S1b in [33] for the slowdown behavior during the 180 days of the data set and how workdays differ from the weekend, and how even Sundays are distinguishable from Saturdays. In Fig. 1 we compare the speed factor distributions over the whole network for the selected time slots: The orange curve is associated with the nocturnal time slot (22 h) and, as expected, it has the highest average speed and the smallest number of edges with slowdowns below 40% of the free flow. We choose this value as a threshold to define congested edges. The morning off-peak distribution (10 h, cyan) shows a considerably slower average speed factor than the evening one and it is globally more similar to the 8 h (blue) and 17 h (red) that are almost indistinguishable in this respect.

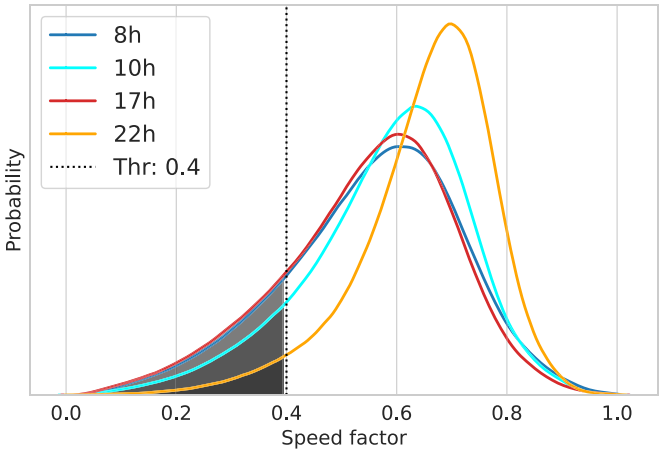

FIG. 1. Uber speed factor distributions. Shaded areas on the left highlight congested edges.

B. Urban network selection and simulation details

To complement the comparisons with real data, we select the vehicular transportation layer of the urban networks of eight large cities (five in Europe, two in the U.S., and one in China) and their surroundings from OpenStreetMap. The cities have been selected to be representative of very different urban structures, stemming from their different history, geographic location, and local site features. The radius of the circle inscribed in each square region is 20 km for all cities except for Rome and Madrid (12 and 15 km, respectively). The number of edges of the corresponding graphs goes from about 1.0×10^5 for Rome to about 5.5×10^5 for London. Detailed information concerning OSM road networks is reported in Table S1 in [33]. The final number of added OD pairs at the end of each simulation is $V = 2.0 \times 10^6$, sufficient to bring all cities to a deeply congested state, as shown in Fig. 3. The computed vehicular speed on each edge is multiplied by a small Gaussian noise $\xi(\mu = 1, \sigma = 0.1)$ to reproduce the intrinsic variability of drivers. All simulations were run with $T = 3600$ s.

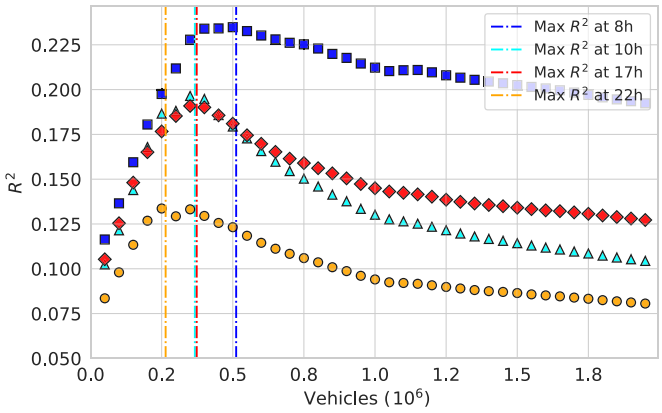

FIG. 2. Edge-level correlation between real speed data (at 8, 10, 17, and 22 h) and simulated speed for increasing traffic volume for London.

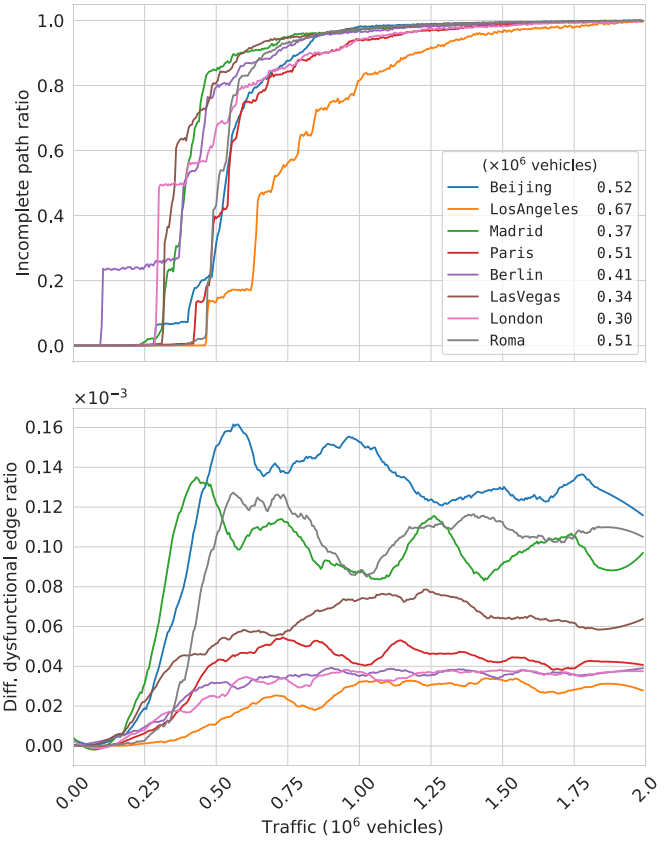

FIG. 3. Simulation. (a) The fraction of incomplete paths follows a sigmoidlike curve as traffic load increases. The V^* is shown in the legend for all cities. Each curve is averaged over five replicas. (b) Fraction of edges removed at each step from city networks. The area under each curve is the total fraction of dysfunctional edges.

C. Percolation analysis

Being able to produce synthetic traffic with adjustable congestion levels, we perform a critical percolation analysis to check open questions about the fragmentation process under stress: The network graph is pruned at increasing speed thresholds to locate the phase transition exactly when the size distribution of the resulting strongly connected subnetworks follows a power law [34]. The critical exponent associated with this transition is supposed to depend, in particular conditions, on traffic intensity, as observed for real-world data sets in large cities such as Beijing [35]. It is also supposed to show metastability during rush hours [36]. The above percolation phase transition is not a property of high congestion alone; it is an indicator of a change in the network behavior visible at all traffic levels, but appearing for different speed thresholds. Within this percolation paradigm, even some of the free-flowing edges of an almost empty network would be classified as dysfunctional at criticality [16,34,35]. On the other hand, when dealing with real traffic congestion, edges are customarily deemed dysfunctional only with road densities approaching their physical limit and diverging travel times [11].

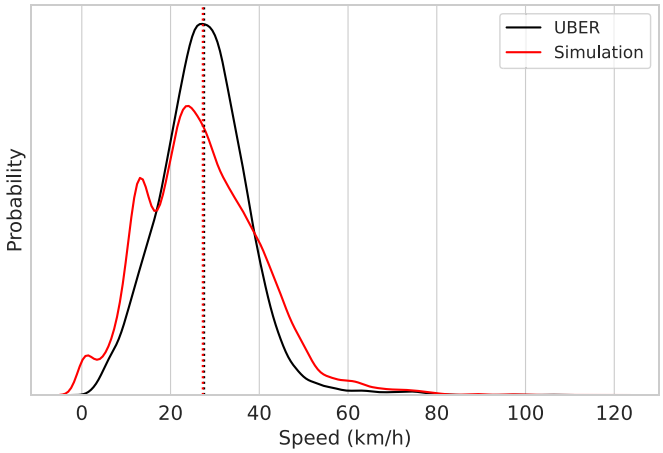

FIG. 4. Speed factor distribution comparison for the real data set (at 8 h) and the simulation (at maximum R^2).

D. Model approximations

The proposed method has been developed to evaluate the effects of adding agent interaction on the network while keeping the model as simple as possible. The known approximations are mainly due to (a) the Greenshields model being very rough, especially for urban traffic, but its simplicity helps the explainability of the results; (b) there being no explicit time evolution as in cellular automata models (e.g., the Nagel-Schreckenberg model), but a sequence of path additions in a *first come, better served* approach; and (c) OD pairs being uniformly extracted, thus preventing us from fully describing the known switch of the average traffic direction from the morning to the evening peak hours [13,37].

E. Comparing the interacting model, BC, and real traffic

We first consider the correlation between the speeds observed in coarse-grained real traffic during the four time slots and those produced by the simulation for increasing volumes of traffic. We use ordinary least squares to compute the coefficient of determination R^2 (square of the Pearson correlation coefficient), which quantifies the ratio of explained variance. In Fig. 2, each correlation curve shows a clear maximum: At 8 h (blue), $R^2 \sim 0.23$ at about $V = 0.5 \times 10^6$ vehicles after a steep growth from lower traffic. After reaching the maximum, the correlation slowly decays to $R^2 \sim 0.2$ for very high congestion. For different time slots, the maximum correlation is lower [e.g., $R^2 \sim 0.2$ at 10 h (cyan) and 17 h (red), while $R^2 \sim 0.13$ at 22 h (orange)] and happens at lower traffic volumes. During off-peak time slots R^2 (red and orange) also decays much more for high simulated traffic. These values should be compared with the highest R^2 obtained for standard BC (used as a load predictor) and real traffic slowdown, which is of the order of 3×10^{-2}. From the same data used for the blue curve (8 h) in Fig. 2, we extract the whole-graph distributions of the real and synthetic speeds to show their similarity, at maximum R^2, in Fig. 4.

Figure 3(a) shows how each urban network reacts to increasing levels of traffic: Most cities behave in a similar way with respect to the fraction of "impossible" paths, i.e., the ones between OD pairs that can be connected only including congested edges, with a sigmoidlike curve that visualizes the progressive network breakup. We refer to the number of vehicles associated with the sigmoid center as the critical traffic volume V^*. Los Angeles (orange curve) appears to be more resistant and its network breaks after adding about 0.7×10^6 vehicles, a fact due in part to the total length of its roads and to the meshlike topology that produces a strong path degeneration (multiple options at a similar cost). Las Vegas (brown), on the other hand, albeit sharing a similar organization, is much smaller and collapses together with the rest of the European cities. Berlin, London, Las Vegas, and Madrid are the first to fail (traffic volume $V \sim 0.35 \times 10^6$), followed by Beijing, Rome, and Paris, resisting up to $V \sim 0.5 \times 10^6$ despite a vastly different total street length within the two groups.

The traffic volume needed to reach maximum R^2 is just above the value necessary to split into two halves the London network in the simulation, as visible in Fig. 3: The pink curve has a small plateau for about $V = 0.3 \times 10^6$ vehicles when all bridges on the River Thames become congested, making it impossible to reach the other side of the city within the chosen T. Figure 3(b) shows the fraction of edges that become dysfunctional at each step and highlights the fact that a very small minority of congested edges can lead to transportation breakdown: Beijing, Rome, and Madrid remain connected with a total fraction (area under each curve) of defects much larger than the other cities. Notably, the two U.S. cities with meshlike geometry collapse with relatively fewer congested edges. In Figs. S22 and S23 in [33] we also report detailed graphs for all cities containing the incomplete path ratio, its flex location, and the curve of the fraction of removed edges at each step.

In Fig. 4 the whole-network speed distribution obtained from our model (at maximum R^2) is compared to the real data set during the morning peak hour; it shows a remarkable overlap between the two curves and almost identical average values. The small superimposed peaks are remnants of the original speed limits on uncongested roads. Figure 5 presents a set of curves showing how the real data (at 8 h), for all edges (speed factor, y axis), are connected to the simulated density (ρ, x axis) at different levels of synthetic traffic: Dark blue symbols correspond to $V \sim 0.2 \times 10^6$ vehicles, light blue to $V \sim 0.5 \times 10^6$, cyan to $V \sim 0.7 \times 10^6$, and red to $V \sim 2.0 \times 10^6$. They are a subset of all points shown for the blue curve in Fig. 2. Open black squares show how poorly the normalized standard BC correlates with the real speed data and how our model with very low traffic (dark blue curve) converges to BC.[1]

After comparing speed distributions and computing their correlation levels, we turn to a qualitative comparison between traffic maps, where each street edge is characterized by a normalized quantity that can be considered a proxy for congestion: (i) load computed by standard BC, (ii) speed factor

[1]The x-axis values refer to the center of bins of either density ρ or standardized BC: Given a specific x value, all edges with ρ (or standardized BC) within the interval $[x - \delta, x + \delta]$ are grouped, then their corresponding Uber speeds are averaged, and the mean value is plotted on the diagram.

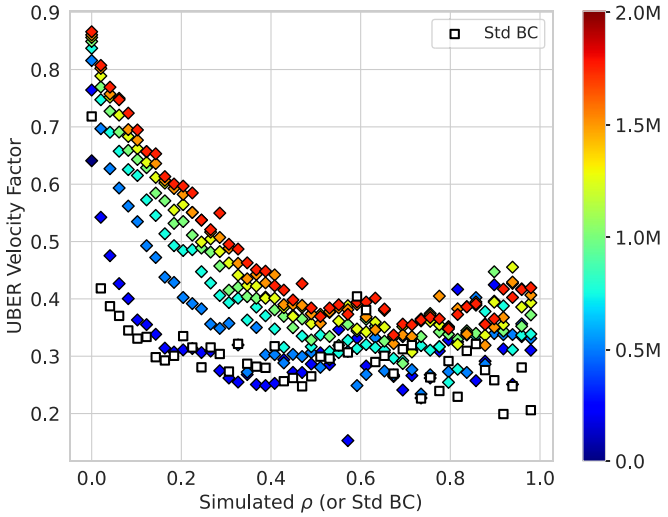

FIG. 5. Real data set (at 8 h) speed factor dependence on simulated ρ for different levels of traffic load (identified by color). Each symbol is the average real speed factor for all edges within a ρ bin. Simulated densities show a correlation for values up to a density of 0.5, whereas the BC is totally uncorrelated after 0.25. For reference, the open black squares show the normalized standard BC prediction.

from the real data set, and (iii) vehicular density from the simulations. In Fig. 6 we compare, side by side, the standard BC, the Uber traffic speed factor during the morning rush hour, and the vehicular density ρ of simulated traffic for the central part of London. The standard BC [Fig. 6(a)] badly underestimates congestion on most edges with respect to the real network state as shown in Fig. 6(b), except for some important arteries that are correctly identified. This behavior is expected since BC does not take into account the interactions and therefore it is not able to describe the progressive traffic spillover towards secondary (but still functional) roads. Figure 6(c) shows that, in our simulations, the traffic volume that correlates the most with the real data at 8 h is $V = 0.5 \times 10^6$, which is approximately 70% above V^* (see Fig. 3). Thus, for the morning peak hour, our model [Fig. 6(c)], qualitatively and quantitatively, far outperforms the BC at describing real traffic patterns. The prediction quality breaks down towards the edges of the simulated area because no transport is simulated outside of it (full map shown in Fig. S10 in [33]). We compare the congestion maps obtained from the simulations for all other cities, for V^* and at half volume $\frac{1}{2}V^*$, along with the BC prediction. The simulation at $\frac{1}{2}V^*$ shows that in a low interaction scenario, the BC qualitatively resembles the results of our model, while at higher traffic levels its pattern is only able to highlight the main roads. It is especially enlightening to observe the results for Los Angeles and Las Vegas, which are characterized by a meshlike topology with a high level of shortest path degeneracy: For low congestion a few roads attract most of the traffic, which then spills over to the alternative routes with equivalent lengths for higher V. The existence of these alternative paths guarantees a higher network resilience but at the cost of exploiting residential areas, which have been reported to already be experiencing a growth in congestion and noise as the use of traffic-aware automatic route planners becomes widespread among drivers [38]. Older European cities behave differently since topology is much more complex and stratified, and residential areas are more protected than their U.S. counterparts by the existence of a deeper road hierarchy, able to sustain the effort during peak hours. All these results are shown in Figs. S2– S9 in [33].

We now turn our attention to the spatial correlation of congestion for both simulated traffic and real data. In Fig. 7 we show the spatial correlation computed by applying Eq. (5) on congestion maps such as those depicted in Fig. 6(b) for Uber data at four time slots, two peak hour and two off-peak hour. It is clear that the correlation follows a power law until the exponential tail discussed in Ref. [27] kicks in for long distances. An interesting result is that the relevant exponent has two regimes: $\gamma \sim 0.2$ for peak hours and $\gamma \sim 0.5$ for off-peak periods. This means that congestion decreases much faster with distance (as usual, measured in travel time on an empty network) for lighter traffic than for heavier traffic. This result goes partially against previous findings that detected no difference in the γ values for different traffic levels [27,30,39].

(a) (b) (c)

FIG. 6. Central London congestion maps: (a) normalized standard BC, (b) real data-set inverse speed factor at 8 h, and (c) simulation traffic density ρ at maximum R^2 (with $V = 0.5 \times 10^6$). Yellow is low road usage and red stands for the 95th percentile for each distribution.

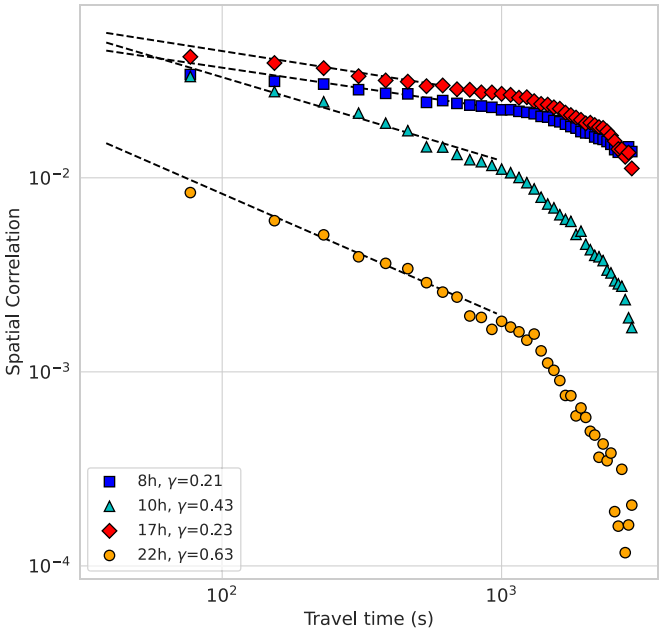

FIG. 7. London spatial correlation of congestion for all four time slots using the Uber data. Regressions are performed on the linear part of the curve and their γ exponents are shown in the legend for each time slot.

Performing the same analysis on the synthetic data shows a trend similar to the real data set as shown in Fig. 8: Steep slopes are associated with low and medium traffic ($\gamma \sim 0.8$ for $V \sim 0.5 \times 10^6$) and flatter profiles with highly congested networks ($\gamma \sim 0.4$ for $V \sim 1.5 \times 10^6$). So the simulation is compatible with the real data for γ in similar traffic scenarios.

The same analysis was performed for all the other cities, for which the spatial correlations show similar behavior to what was observed for London: In most cases, γ decreases

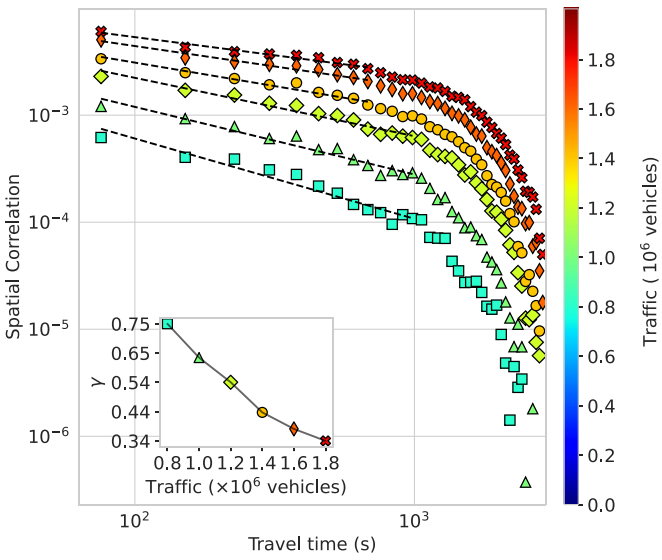

FIG. 8. Simulation (London) of the spatial correlation of congestion for increasing traffic load. Linear regressions and the associated γ exponents are computed for the linear part of the curve and the γ dependence on traffic level is shown in the inset.

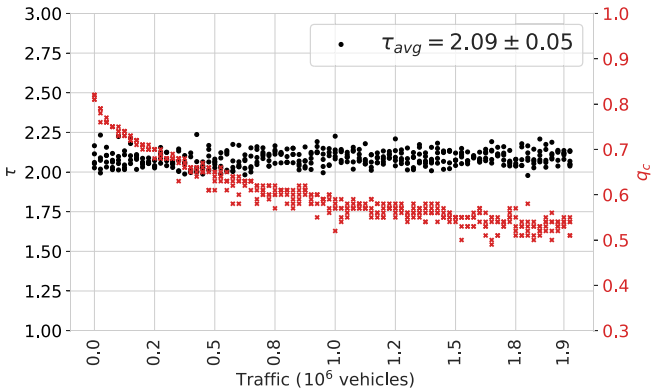

FIG. 9. Simulation (London) of the critical speed factor q_c (red) and critical exponent τ (black) for increasing levels of traffic load. Multiple points for the same abscissa represent different replicas. Here τ_{avg} is the average over the whole domain for all replicas.

linearly with growing traffic except for Beijing, for which we see an abrupt regime switch, from $\gamma \sim 0.4$ for $V \sim 0.6 \times 10^6$ to a constant $\gamma \sim 0.2$ for higher V. More details about the spatial correlations and the associated cocongestion probabilities are presented in Figs. S17– S21 in [33].

The last comparison between real and simulated traffic regards percolation results. Percolation offers an insightful picture of the weaknesses of the network when considering speeds above a certain threshold q_c before reaching the maximum capacity of the edges. On the other hand, the study of the progressive appearance of dysfunctional edges with increasing traffic volume (as shown in Fig. 3) only focuses on the way in which more and more paths become impossible.

For each traffic level, both real and synthetic, we first compute the critical speed factor q_c (details on the percolation method are given in [33]) at which the size distribution of the graph-connected components becomes a power law. Once q_c is known, a linear regression produces the τ value. In Fig. 9 we see that τ stays almost constant over the whole range of simulated traffic volumes and its average value is $\tau_{\text{avg}} = 2.09 \pm 0.05$, a result that agrees with the theoretical value for isotropically directed graphs of $\tau \sim 2.1$ [40]. This result is slightly above the value obtained for real traffic data: τ varies very little for extremely different congestion states and stays just below 2.0 as shown in Table I. The critical threshold speed factor q_c for the simulations, on the other hand, decreases from about $q_c \sim 0.8$ for no congestion to $q_c \sim 0.55$ for a saturated network. These values approximate well what we observe

TABLE I. Critical speeds and critical exponents for cluster size distribution and for spatial correlation measured at four time slots for the Uber data set for London.

Time	q_c	τ	γ
8–9	0.54 ± 0.05	1.95 ± 0.03	0.21 ± 0.05
10–11	0.58 ± 0.02	1.99 ± 0.03	0.43 ± 0.05
17–18	0.51 ± 0.02	1.96 ± 0.03	0.23 ± 0.05
22–23	0.66 ± 0.01	1.96 ± 0.02	0.63 ± 0.05

for real traffic: $q_c \sim 0.58$ (0.66) for off-peak hours and $q_c \sim 0.54$ (0.51) for peak hours, for morning (afternoon) time slots.

The main result here is that we observe no clear τ dependence on traffic volume for London, for both simulations and real traffic; moreover, their q_c trend shows good agreement. Most of the other cities have very small τ dependence on traffic volume and its average value agrees with the theoretical prediction of $\tau \sim 2.1$ with two notable exceptions: (i) Los Angeles starts from $\tau \sim 2.15$ for low traffic but rises to $\tau \sim 2.2$ for high V and (2) Beijing, on the other hand, has a baseline $\tau \sim 2.0$ but has at least one clear peak occurring for low to medium traffic volumes with $\tau \sim 2.3$ for all replicas. For Beijing, q_c confirms this anomaly with a clear dip at the same traffic volume. This could be related to the previous results of Ref. [35] in which a switch for τ was observed between peak hours and off-peak time slots with values similar to ours. This result needs further analysis, but it would be very interesting if such a dynamical effect could be predicted just by starting from city maps. Berlin showed another interesting behavior: τ starts with a relatively high value of approximately 2.1 up to $V \sim 0.5 \times 10^6$, where it clearly drops to $\tau \sim 2.0$ and then stabilizes to approximately 2.05 afterward. This dip in τ is also visible for q_c and is associated with a strong increase in replica variability. See Figs. S11–S14 in [33] for the detailed graphs of all cities.

IV. CONCLUSION

In this work we introduced a simple model to predict network activity at the edge level. Our method is inspired by a known and intuitive method to approximate BC, but also introduces a repulsive term preventing unphysical densities. This approach leads to dynamically evolving fastest paths, which are progressively attracted towards uncongested parts of the network, as the total traffic volume increases. This simulation scheme is particularly fit to describe the network loading phase leading to peak congestion.

We extensively compared our predictions for the Greater London area to massive measured data of real traffic speeds, finding notable agreement in particular for speed distributions over the whole network at specific time slots. The qualitative accord for congestion maps is confirmed by edge-level speed correlation. The simulations show that our model is able to grasp important structural properties of real urban traffic, as confirmed by a coherent trend in the spatial correlation behavior of congested edges and the associated critical exponent, with respect to traffic volume. Encouraged by these results, we finally applied percolation analysis to real and synthetic traffic by comparing the Fisher exponent values, at different times, associated with network fragmentation under load, finding very good agreement. Synthetic experiments were carried out on a variety of different road networks for several kinds of cities.

Despite not trying to accurately simulate vehicular traffic in the urban context and explicitly choosing a very coarse vehicular model, the result is a usable tool to quickly compare different city organizations both for testing theoretical ideas and for getting useful glimpses of the main breakup modes of urban networks. Also note that, even though we decided to apply our method to predict congestion patterns typical of urban vehicular traffic, it is expected that other transport phenomena involving agent competition for network resources could be approached in a similar way. In particular, we expect that analyses where BC has provided important insights, such as those on power grids, the internet backbone, air travel, and maritime cargo shipping [2–5], might benefit from our refined approach.

ACKNOWLEDGMENTS

We are deeply indebted to Enrico Gobbetti and Francesco Versaci for the many useful discussions. We acknowledge the contribution of Sardinian Regional Authorities under project XDATA (art 9 L.R. 20/2015).

[1] D. R. White and S. P. Borgatti, Betweenness centrality measures for directed graphs, Social Netw. **16**, 335 (1994).
[2] M. Barthélemy, Spatial networks, Phys. Rep. **499**, 1 (2011).
[3] P. Holme, Congestion and centrality in traffic flow on complex networks, Adv. Complex Syst. **06**, 163 (2003).
[4] R. Guimera, S. Mossa, A. Turtschi, and L. A. Nunes Amaral, The worldwide air transportation network: Anomalous centrality, community structure, and cities' global roles, Proc. Natl. Acad. Sci. USA **102**, 7794 (2005).
[5] A. Kazerani and S. Winter, in *Proceedings of the 12th AGILE International Conference on Geographic Information Science, Hannover, 2009*, edited by J.-H. Haunert, B. Kieler, and J. Milde (Springer, Berlin, 2009), pp. 1–9.
[6] L. C. Freeman, S. P. Borgatti, and D. R. White, Centrality in valued graphs: A measure of betweenness based on network flow, Social Netw. **13**, 141 (1991).
[7] T. Agryzkov, L. Tortosa, and J. F. Vicent, A variant of the current flow betweenness centrality and its application in urban networks, Appl. Math. Comput. **347**, 600 (2019).
[8] S. Gao, Y. Wang, Y. Gao, and Y. Liu, Understanding urban traffic-flow characteristics: A rethinking of betweenness centrality, Environ. Plann. B **40**, 135 (2013).
[9] M. Cogoni, G. Busonera, and G. Zanetti, Ultrametricity of optimal transport substates for multiple interacting paths over a square lattice network, Phys. Rev. E **95**, 030108(R) (2017).
[10] C. H. Yeung and D. Saad, Competition for shortest paths on sparse graphs, Phys. Rev. Lett. **108**, 208701 (2012).
[11] H. Hamedmoghadam, M. Jalili, H. L. Vu, and L. Stone, Percolation of heterogeneous flows uncovers the bottlenecks of infrastructure networks, Nat. Commun. **12**, 1254 (2021).
[12] L. E. Olmos, S. Çolak, S. Shafiei, M. Saberi, and M. C. González, Macroscopic dynamics and the collapse of urban traffic, Proc. Natl. Acad. Sci. USA **115**, 12654 (2018).
[13] S. Çolak, A. Lima, and M. C. González, Understanding congested travel in urban areas, Nat. Commun. **7**, 10793 (2016).

[14] H. Youn, M. T. Gastner, and H. Jeong, Price of anarchy in transportation networks: Efficiency and optimality control, Phys. Rev. Lett. **101**, 128701 (2008).
[15] Y. Ren, M. Ercsey-Ravasz, P. Wang, M. C. González, and Z. Toroczkai, Predicting commuter flows in spatial networks using a radiation model based on temporal ranges, Nat. Commun. **5**, 5347 (2014).
[16] D. Li, B. Fu, Y. Wang, G. Lu, Y. Berezin, H. E. Stanley, and S. Havlin, Percolation transition in dynamical traffic network with evolving critical bottlenecks, Proc. Natl. Acad. Sci. USA **112**, 669 (2015).
[17] A. Kirkley, H. Barbosa, M. Barthelemy, and G. Ghoshal, From the betweenness centrality in street networks to structural invariants in random planar graphs, Nat. Commun. **9**, 2501 (2018).
[18] C. Bongiorno, Y. Zhou, M. Kryven, D. Theurel, A. Rizzo, P. Santi, J. Tenenbaum, and C. Ratti, Vector-based pedestrian navigation in cities, Nat Comput Sci **1**, 678 (2021).
[19] M. Lee, H. Barbosa, H. Youn, P. Holme, and G. Ghoshal, Morphology of travel routes and the organization of cities, Nat. Commun. **8**, 2229 (2017).
[20] A. Diet and M. Barthelemy, Towards a classification of planar maps, Phys. Rev. E **98**, 062304 (2018).
[21] D. Helbing, Traffic and related self-driven many-particle systems, Rev. Mod. Phys. **73**, 1067 (2001).
[22] D. Aldous and K. Ganesan, True scale-invariant random spatial networks, Proc. Natl. Acad. Sci. USA **110**, 8782 (2013).
[23] M. E. J. Newman, A measure of betweenness centrality based on random walks, Social Netw. **27**, 39 (2005).
[24] H. Rakha and B. Crowther, Comparison of Greenshields, pipes, and Van Aerde car-following and traffic stream models, Transp. Res. Record **1802**, 248 (2002).
[25] M. Riondato and E. M. Kornaropoulos, Fast approximation of betweenness centrality through sampling, Data Min. Knowl. Disc. **30**, 438 (2016).
[26] W.-L. Jin, *Introduction to Network Traffic Flow Theory: Principles, Concepts, Models, and Methods* (Elsevier, Amsterdam, 2021).
[27] E. Taillanter and M. Barthelemy, Empirical evidence for a jamming transition in urban traffic, J. R. Soc. Interface **18**, 20210391 (2021).
[28] T. A. Witten Jr., and L. M. Sander, Diffusion-limited aggregation, a kinetic critical phenomenon, Phys. Rev. Lett. **47**, 1400 (1981).
[29] A. Cavagna, A. Cimarelli, I. Giardina, G. Parisi, R. Santagati, F. Stefanini, and M. Viale, Scale-free correlations in starling flocks, Proc. Natl. Acad. Sci. USA **107**, 11865 (2010).
[30] G. Petri, P. Expert, H. J. Jensen, and J. W. Polak, Entangled communities and spatial synchronization lead to criticality in urban traffic, Sci. Rep. **3**, 1798 (2013).
[31] Uber Technologies, Inc., Uber movement, https://movement.uber.com/ (2019).
[32] Map data are copyrighted by OpenStreetMap contributors and are available at www.openstreetmap.org
[33] See Supplemental Material at http://link.aps.org/supplemental/10.1103/PhysRevE.109.044302 DOI for details.
[34] M. Cogoni and G. Busonera, Stability of traffic breakup patterns in urban networks, Phys. Rev. E **104**, L012301 (2021).
[35] G. Zeng, D. Li, S. Guo, L. Gao, Z. Gao, H. E. Stanley, and S. Havlin, Switch between critical percolation modes in city traffic dynamics, Proc. Natl. Acad. Sci. USA **116**, 23 (2019).
[36] G. Zeng, J. Gao, L. Shekhtman, S. Guo, W. Lv, J. Wu, H. Liu, O. Levy, D. Li, Z. Gao, H. E. Stanley, and S. Havlin, Multiple metastable network states in urban traffic, Proc. Natl. Acad. Sci. USA **117**, 17528 (2020).
[37] M. Mazzoli, A. Molas, A. Bassolas, M. Lenormand, P. Colet, and J. J. Ramasco, Field theory for recurrent mobility, Nat. Commun. **10**, 3895 (2019).
[38] R. C. Batac and M. T. Cirunay, Shortest paths along urban road network peripheries, Physica A **597**, 127255 (2022).
[39] L. Daqing, J. Yinan, K. Rui, and S. Havlin, Spatial correlation analysis of cascading failures: Congestions and blackouts, Sci. Rep. **4**, 5381 (2014).
[40] A. W. T. de Noronha, A. A. Moreira, A. P. Vieira, H. J. Herrmann, J. S. Andrade, and H. A. Carmona, Percolation on an isotropically directed lattice, Phys. Rev. E **98**, 062116 (2018).